

Stone–Wales transformation in boron nitride nanotubes

J. Song,^a H. Jiang,^b J. Wu,^c Y. Huang^{a,*} and K.-C. Hwang^c

^aDepartment of Mechanical Science and Engineering, University of Illinois at Urbana-Champaign, Urbana, IL 61801, USA

^bDepartment of Mechanical and Aerospace Engineering, Arizona State University, Tempe, AZ 85287, USA

^cDepartment of Engineering Mechanics, Tsinghua University, Beijing 100084, China

Received 12 April 2007; revised 8 June 2007; accepted 16 June 2007

Available online 13 July 2007

A hybrid atomistic/continuum model is used to study the Stone–Wales transformation (90° rotation of an atomic bond) in boron nitride nanotubes (BNNTs) subjected to tension. The critical strain for Stone–Wales transformation is 11.47% for (5, 5) armchair and 14.23% for (10, 0) zigzag BNNTs, which agree well with the atomistic simulations. The critical strain depends on the BNNT chirality for small tube radius, but this dependence gradually disappears with the increasing tube radius.

© 2007 Acta Materialia Inc. Published by Elsevier Ltd. All rights reserved.

Keywords: Stone–Wales transformation; Boron nitride nanotube; Defects

Boron nitride nanotubes (BNNTs) possess unique mechanical, thermal, electrical and chemical properties, and represent an important class of nanotubes. Their tensile stiffness [1–6] is comparable to that of carbon nanotubes. They have high thermal conductivity along the nanotube [7], and good resistance to oxidation at high temperature [8]. However, in contrast to carbon nanotubes, BNNTs always have large band gaps, and are therefore semiconductors, regardless of the chirality and diameter [9].

Atomistic simulations [10–13] and experiments [14] have shown topological defects (5775) in BNNTs which correspond to the 90° rotation of a boron nitride bond. This is called the Stone–Wales transformation, which generates two unfavorable homoelemental (boron–boron and nitrogen–nitrogen) bonds. Figure 1 shows the schematic diagrams of 5775 defects in (*n, n*) armchair BNNTs (Fig. 1a) and in (*n, 0*) zigzag BNNTs with clockwise (Fig. 1b) and counterclockwise (Fig. 1c) bond rotation. In contrast to carbon nanotubes, the clockwise and counterclockwise bond rotations in BNNTs give different states of energy [11,12,15,16]. Only for (*n, n*) armchair BNNTs do the clockwise and counterclockwise bond rotations become the same.

Jiang et al. [17] and Song et al. [18] developed a hybrid atomistic/continuum model based on the

interatomic potential for carbon [19] to study the Stone–Wales transformation in carbon nanotubes under tension. The critical tensile strain for the Stone–Wales transformation is about 5% for the (5, 5) armchair and 10% for the (10, 0) zigzag carbon nanotubes, which agree well with the atomistic simulations [20]. It is unclear whether this hybrid atomistic/continuum model works for other nanostructured materials such as BNNTs, which involve two different atoms (boron and nitrogen).

The aim of this paper is to extend the hybrid atomistic/continuum model for BNNTs and to study the Stone–Wales transformation. For boron nitride, Albe et al. [21] established an interatomic potential

$$V(r_{ij}; \theta_{ijk}) = V_R(r_{ij}) - B_{ij}V_A(r_{ij}), \quad (1)$$

where V_R and V_A are the repulsive and attractive pair terms that depend only on the distance r_{ij} between a pair of atoms i and j , and B_{ij} represents the multibody coupling that depends on neighboring atoms through bond angle. The detailed expressions for V_R , V_A and B_{ij} [21], as summarized in [6], are much more complex than their counterparts for carbon nanotubes [19] since the index pair i and j can be boron–nitrogen, nitrogen–nitrogen, and boron–boron.

This paper is summarized as follows. The hybrid atomistic/continuum model is first developed for BNNTs, based on the interatomic potential [21], to study the Stone–Wales transformation in BNNTs under tension. The model is compared with the limited atomistic simulation results [10–12], and is then used

* Corresponding author. Tel.: +1 217 265 5072; fax: +1 217 244 6534; e-mail: huang9@uiuc.edu

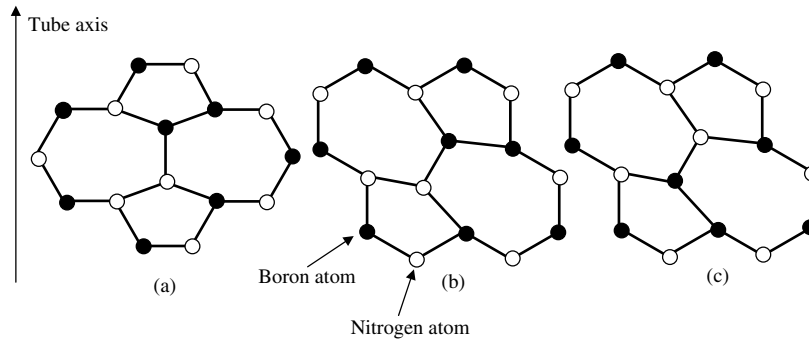


Figure 1. Schematic diagrams of (a) a 5775 defect in an (n,n) armchair BNNT; (b) a 5775 defect induced by clockwise bond rotation in an $(n,0)$ zigzag BNNT; (c) a 5775 defect induced by counterclockwise bond rotation in an $(n,0)$ zigzag BNNT. The solid and open circles represent boron and nitrogen atoms, respectively.

to systematically study the effect of BNNT diameter and chirality on the Stone–Wales transformation.

Figure 2 shows a schematic diagram of the hybrid atomistic/continuum model for the Stone–Wales transformation in BNNTs. The 90° rotation of a boron–nitrogen bond is highlighted in Figure 2.

The atoms on a BNNT are divided into two groups. Group (i) contains atoms far away from the rotated bond. Atoms in this group undergo relatively uniform deformation since the effect of bond rotation is rather localized. Their positions are determined by the continuum model for BNNTs [6], as discussed below. Group (ii) contains atoms in the vicinity of the rotated bond. Atoms in this group undergo nonuniform deformation due to bond rotation. Their positions are to be determined by molecular mechanics in order to minimize the total energy of the system. The conjugate gradient

method provided by the IMSL program [22] is adopted to minimize the total energy.

For the relative uniform deformation of Group (i) atoms, Song et al. [6] established a continuum theory based on the interatomic potential [21]. A BNNT is composed of a triangular lattice of boron atoms and another of nitrogen atoms. The atoms in each lattice follow Cauchy–Born rule [23,24], but two lattices may undergo a shift vector ζ [6] in order to reach equilibrium. The bond length and angle can be obtained in terms of the Green strain E and shift vector ζ . The Cauchy–Born rule then gives the strain energy density W in the continuum analysis in terms of E and ζ via the interatomic potential, i.e., $W = W(E, \zeta)$. The shift vector ζ plays the role of relaxing atoms between two lattices in order to ensure equilibrium of atoms via energy minimization, $\partial W / \partial \zeta = 0$, which gives the shift vector ζ in terms of E ,

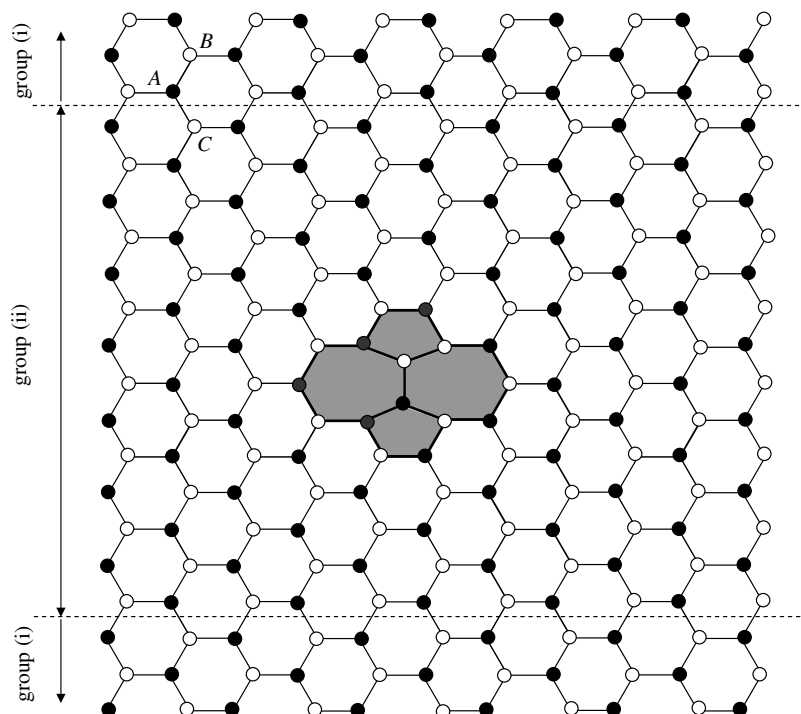
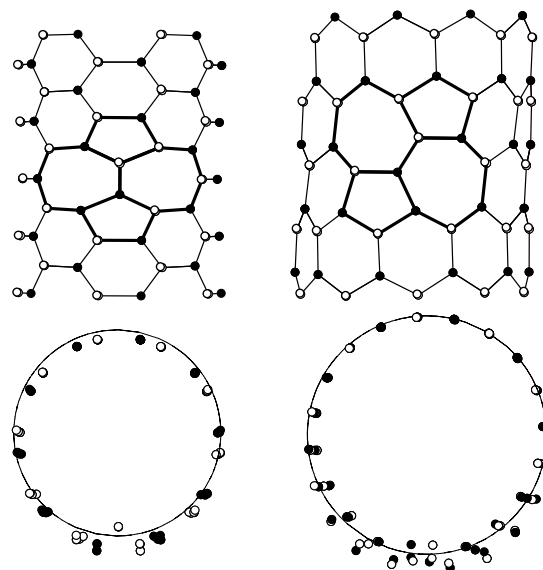


Figure 2. A hybrid atomistic/continuum model for studying the Stone–Wales transformation in armchair BNNTs, where the atoms around the rotated bond are highlighted.

$\zeta = \zeta(E)$. The strain energy density then becomes $W = W[E, \zeta(E)]$. The second Piola–Kirchhoff stress T is the work conjugate of the Green strain, i.e., $T = \partial W / \partial E$.

The atom positions in Group (i) are imposed as the boundary conditions for the determination of atom positions in Group (ii). It is important to point out that, even though atoms are divided to two groups, the total energy of the system cannot be divided because of the multibody nature of atomistic interactions. For example, even though atoms A and B are both in Group (i), as shown in Figure 2, the energy stored in the AB bond depends on the position of atom C in Group (ii). It is important to account for the energy stored in all atomic bonds that is influenced by atoms in Group (ii). In addition, there must be sufficient number of layers of atoms in Group (ii) (in the vicinity of the rotated bond) to ensure the results are accurate.

Figure 3 shows the difference in energy with and without bond rotation, ΔE , versus the tensile strain ε for the (5,5) armchair and (10,0) zigzag BNNTs. Around $\varepsilon = 0$, ΔE is positive such that the perfect BNNT is energetically favorable. As ε increases, ΔE decreases and eventually reaches zero, at which the BNNT with a 5775 defect becomes energetically favorable. For the (5,5) armchair BNNT, the critical strain at which $\Delta E = 0$ is 11.47%, which suggests that the Stone–Wales transformation may occur once the tensile strain exceeds 11.47%. For the (10,0) zigzag BNNT, the critical strain for the counterclockwise 5775 defect (Fig. 1c) is 14.23%, which is smaller than its counterpart 15.08% for the clockwise 5775 defect (Fig. 1b). This is consistent with the ab initio calculations [11] and other molecular mechanics simulations [16]. The critical strains for the Stone–Wales transformation, 11.47% for the (5,5) armchair and 14.23% for the (10,0) zigzag BNNTs, agree well with ab initio calculations [10–12] that reported 12% for (5,5) armchair and 16% for (10,0) zigzag BNNTs.



(a) (5,5) BNNT (b) (10,0) BNNT

Figure 4. Front and top view of 5775 defects in (a) an (5,5) armchair BNNT and (b) a (10,0) zigzag BNNT with counterclockwise 5775 bond rotation.

Table 1. Effect of BNNT chirality and radius on the critical strain for the Stone–Wales transformation

Armchair BNNT			Zigzag BNNT		
(n,n)	Radius (nm)	Critical strain (%)	(n,0)	Radius (nm)	Critical strain (%)
(5,5)	0.354	11.47	(9,0)	0.367	14.36
(6,6)	0.423	11.72	(10,0)	0.409	14.23
(7,7)	0.492	11.89	(12,0)	0.488	14.04
(8,8)	0.561	12.08	(14,0)	0.568	13.87
(10,10)	0.700	12.35	(18,0)	0.728	13.53

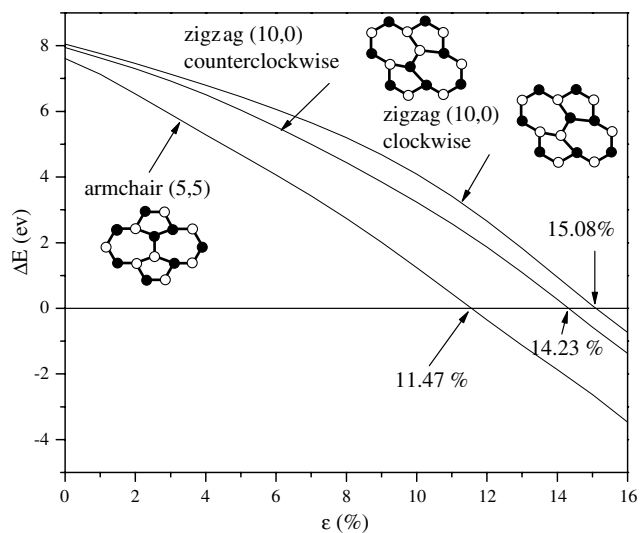


Figure 3. The energy difference ΔE versus the tensile strain ε for (5,5) armchair and (10,0) zigzag BNNTs. Here $\Delta E = E - E_{\text{perfect}}$ is the difference between the energy for systems with and without Stone–Wales transformation.

The Stone–Wales transformation breaks the perfect atomic structure of nanotubes, which may significantly reduce their electrical and thermal conductivity and other superior properties [25–28]. Figure 4 shows the front and top view of 5775 defects in the (5,5) armchair and (10,0) zigzag BNNTs (with counterclockwise bond rotation). The boron and nitrogen atoms clearly do not stay on a cylindrical surface anymore due to the Stone–Wales transformation. The maximum displacement of atoms (from the cylindrical surface) is 0.056 nm for the (5,5) armchair BNNT and 0.057 nm for the (10,0) zigzag BNNT.

Table 1 shows the effect of BNNT chirality and radius on the critical strain for the Stone–Wales transformation. At approximately the same BNNT radius, the critical strain for armchair BNNTs is always smaller than that for zigzag BNNTs. This dependence on the BNNT chirality decreases as the tube radius increases. For example, the difference between the critical strains for (5,5) and (9,0) BNNTs (approximately the same radii) is 2.89%, while the difference decreases to 1.18% between (10,10) and (18,0) BNNTs (approximately the same radii).

We have used a hybrid atomistic/continuum model to study the Stone–Wales transformation in boron nitride nanotubes subject to tension. It is shown that the Stone–Wales transformation occurs and generates the 5775 defects when the tensile strain reaches 11.47% for (5,5) armchair and 14.23% for (10,0) zigzag BNNTs. The critical strain depends on the BNNT chirality for small tube radius but this dependence gradually disappears with the increasing tube radius.

Y.H. acknowledges the support from NSF (grants 00-99909, 01-03257, and 03-28162 via the Nano-CEMMS Center at UIUC), Office of Naval Research (grant N00014-01-1-0205, Program Manager Dr. Y.D.S. Rajapakse), and NSFC. K.C.H. acknowledges support from NSFC and the Ministry of Education, China.

- [1] E. Hernández, C. Goze, P. Bernier, A. Rubio, *Phys. Rev. Lett.* 80 (1998) 4502.
- [2] E. Hernández, C. Goze, P. Bernier, A. Rubio, *Appl. Phys. A* 68 (1999) 287.
- [3] N.G. Chopra, A. Zettl, *Solid State Commun.* 105 (1998) 297.
- [4] K.N. Kudin, G.E. Scuseria, B.I. Yakobson, *Phys. Rev. B* 64 (2001) 235406.
- [5] A.P. Suryavanshi, M.F. Yu, J.G. Wen, C.C. Tang, Y. Bando, *Appl. Phys. Lett.* 84 (2004) 2527.
- [6] J. Song, Y. Huang, H. Jiang, K.C. Hwang, M.F. Yu, *Int. J. Mech. Sci.* 48 (2006) 1197.
- [7] C.W. Chang, W.Q. Han, A. Zettle, *Appl. Phys. Lett.* 86 (2005) 173102.
- [8] Y. Chen, J. Zou, S.J. Campbell, G.L. Caer, *Appl. Phys. Lett.* 84 (2004) 2430.
- [9] X. Blase, A. Rubio, S. Louie, M. Cohen, *Europhys. Lett.* 28 (1994) 335.
- [10] H.F. Bettinger, T. Dumitrică, G.E. Scuseria, B.I. Yakobson, *Phys. Rev. B* 65 (2002) 041406.
- [11] T. Dumitrică, H.F. Bettinger, G.E. Scuseria, B.I. Yakobson, *Phys. Rev. B* 68 (2003) 085412.
- [12] T. Dumitrică, B.I. Yakobson, *Phys. Rev. B* 72 (2005) 035418.
- [13] W.H. Moon, H.J. Hwang, *Nanotechnology* 15 (2004) 431.
- [14] Y. Miyamoto, A. Rubio, S. Berber, M. Yoon, D. Toanek, *Phys. Rev. B* 69 (2004) 121413.
- [15] P. Zhang, V. Crespi, *Phys. Rev. B* 62 (2000) 11050.
- [16] W.H. Moon, H.J. Hwang, *Physica E* 28 (2005) 419.
- [17] H. Jiang, X.Q. Feng, Y. Huang, K.C. Hwang, P.D. Wu, *Comput. Methods Appl. Mech. Eng.* 193 (2004) 3419.
- [18] J. Song, H. Jiang, D.L. Shi, X.Q. Feng, Y. Huang, M.F. Yu, K.C. Hwang, *Int. J. Mech. Sci.* 48 (2006) 1464.
- [19] D.W. Brenner, *Phys. Rev. B* 42 (1990) 9458.
- [20] M.B. Nardelli, B.I. Yakobson, J. Bernholc, *Phys. Rev. Lett.* 81 (1998) 4656.
- [21] K. Albe, W. Möller, K.H. Heinig, *Radiat. Eff. Defects Solids* 141 (1997) 85.
- [22] IMSL Fortran 90 MP Library Version 4.01. McGraw-Hill, San Ramon, 1999.
- [23] M. Born, K. Huang, *Dynamical Theory of the Crystal Lattices*, Oxford University Press, Oxford, 1954.
- [24] F. Milstein, *J. Mater. Sci.* 15 (1980) 1071.
- [25] H.J. Choi, J. Ihm, S.G. Louie, M.L. Cohen, *Phys. Rev. Lett.* 84 (2000) 2917.
- [26] D. Tekleab, D.L. Carroll, G. Samsonidze, B.I. Yakobson, *Phys. Rev. B* 64 (2001) 035419.
- [27] R.J. Baierle, S.B. Fagan, R. Mota, A.J.R. Da Silva, A. Fazzio, *Phys. Rev. B* 64 (2001) 085413.
- [28] T.M. Schmidt, R.J. Baierle, P. Piquini, A. Fazzio, *Phys. Rev. B* 67 (2003) 113407.